Liquid−Liquid Phase Separations in Urate Oxidase/PEG Mixtures: Characterization and Implications for Protein Crystallization

D. Vivarès[†,‡,§] and F. Bonneté*[,†]

CRMCN-CNRS, Campus de Luminy, Case 913, F-13288 Marseille Cedex 09, France, and LMCP-UMR7590, Case 115, 4 place Jussieu, F-75252 Paris Cedex 05, France

Received: November 17, 2003; In Final Form: February 25, 2004

In a previous paper (Vivarès, D.; Bonneté, F. *Acta Crystallogr., Sect. D* **2002**, *58*, 472), protein−protein interactions of *Aspergillus flavus* urate oxidase (Uox) in solution were determined by small-angle X-ray scattering in the presence of different poly(ethylene glycol)s (PEG) in order to correlate second virial coefficient measurements with crystallization conditions. In this paper, we have characterized the experimental phase diagram of urate oxidase in the case of PEG 8000 by determining the solubility curve and the dilute part of the liquid−liquid phase separation (LLPS). Within this phase diagram, different mechanisms of urate oxidase crystal growth and LLPS can be observed by optical video microscopy. The influence of the LLPS on both the mechanisms and kinetics of urate oxidase crystal growth was observed by optical microscopy and small-angle X-ray scattering (SAXS). Interactions between the macromolecules were studied by SAXS in the dilute and dense phases of the demixed solution. It was observed that the LLPS precedes and slows down the crystallization. This study shows that urate oxidase is a good model to study protein/PEG mixtures in the general context of protein crystallization.

1. Introduction

Intensive efforts and progress have been made for about 20 years in biomolecule crystallization to move this interdisciplinary area from art to science by a better understanding of nucleation and crystallization mechanisms.[1−3] Applications for a better-controlled crystallization process are numerous. In structural biology and especially in proteomics, it is still one of the main limiting hurdles for X-ray crystallography; in materials science, it can be used for making nanoscale arrays[4] and in pharmaceuticals for the production of drugs;[5] from a medical point of view, protein crystallization can also be the cause of human diseases, for example, congenital human cataracts.[6]

It is now admitted that phase transitions such as liquid−solid (crystal or precipitate) or liquid−liquid (demixion) phase separations are governed by weak interaction forces between molecules in solution:[7,8] Coulombic repulsion, hard-sphere repulsion, and van der Waals attraction... New physics developed in the 1990s, permitting a better understanding of rules that govern crystallization through the study of interactions between macromolecules in solution. This led to more rational successful crystallization trials and good-quality crystals. The first studies performed on lysozyme by SAXS or static light scattering showed a close correlation between the increase in attractive interactions and the decrease in lysozyme solubility when salt is added.[9,10] In parallel, George and Wilson proposed a predictive tool for protein crystallization—the second virial coefficient, which is negative for attractive interactions and was found in a restrictive slot, the so-called "crystallization slot", for favorable crystallization solvent conditions.[11] Since then, numerous biological systems have been studied by different techniques (static light scattering, X-ray or neutron scattering, analytical ultracentrifugation or self-interaction chromatography), allowing the determination of second virial coefficients as a function of various physicochemical parameters, which makes it possible to determine crystallization conditions.[12−21]

Recent experimental and theoretical work pointed out that an LLPS can affect the whole crystallization process and in particular the nucleation mechanism.[22−26] Depending upon the range of the interparticle pair potential, the LLPS can be stable or metastable toward the solubility curve.[23,27] Ten Wolde and Frenkel[23] have shown by numerical simulations that the nucleation rate can be enhanced around the metastable critical point whereas below or above this critical point the energy nucleation barrier is higher. At the same time, Haas and Drenth have proposed, from a thermodynamic model, that nucleation occurs mostly via a two-step mechanism where the first step is a liquid−liquid phase separation giving rise to protein-rich droplets in which, in a second step, crystals can nucleate and grow.[24] Although few experimental work has been done, two studies performed on lysozyme in aqueous salt solutions as a function of temperature have shown that the nucleation rate is enhanced around the liquid−liquid phase boundary[22,25] and then decreases beyond it.[25] Macroscopic liquid−liquid phase separations can also occur in colloid (or protein)−polymer mixtures. A nonadsorbing polymer such as poly(ethylene glycol), added to a colloidal or a protein suspension, induces an attractive interaction between colloidal particles called the depletion potential. Depletion attraction, an entropically driven force, was first described by Asakura and Oosawa[28] and by Vrij.[29] More recently, the phase diagram of colloid−polymer mixtures and the respective positions of the liquid−liquid and liquid−solid phase transitions have been predicted.[30−32] In the special case of protein−polymer mixtures, PEG is also known to induce

* Corresponding author. E-mail: bonnete@crmcn.univ-mrs.fr. Tel: +33 662 922 839. Fax: +33 491 418 916.

† CRMCN (associated with Aix-Marseille II & III Universities).

‡ LMCP-UMR7590.

§ Present address: Center for Molecular and Engineering Thermodynamics, Department of Chemical Engineering, 150 Academy Street, University of Delaware, Newark, Delaware 19716.

10.1021/jp037502u CCC: $27.50
Published on Web 04/28/2004

depletion attractive interactions between proteins and therefore to favor protein crystallization.[16,17,21,33−38] However very few experimental data are available on LLPS in protein/PEG mixtures[39,40] and on its effect on protein crystallization.[37,38]

In previous works, we have studied a new model protein, urate oxidase from *Aspergillus* flavus, a large homotetrameric protein of 128 kDa molecular mass. We have characterized the attractive interactions between protein molecules induced when PEG is added and have correlated them with the urate oxidase crystallization.[17,41,42] In the following text, we characterize the whole urate oxidase/PEG 8000 phase diagram by determining the protein solubility curve and the LLPS boundary, and we study the effect of their respective position on the urate oxidase crystallization mechanisms. Over the whole range of PEG 8000 and protein concentrations studied, the LLPS turned out to be metastable toward the solubility curve. Optical video-microscopy observations enabled us to characterize different LLPS morphologies (droplets or a bicontinuous network). In parallel, we have also performed some SAXS experiments to get additional information on the LLPS microstructures and in particular on the protein−protein interactions in the protein-poor and the protein-rich phases. Molecules of urate oxidase in the protein-poor phase appeared to be in an attractive regime, but the protein-rich phase turned out to be a strong and repulsive dense phase. Furthermore, beyond the LLPS boundary, optical microscopy revealed that the LLPS precedes and slows down the protein crystal growth, which can be explained by considering the composition of the dense and the light phases.

2. Materials and Methods

2.1. Solutions. Urate oxidase (complexed with 8-azaxanthine) solution was prepared as described in a previous paper[17] and put in a 50 mM Tris buffer at pH 8.5. The protein solution was concentrated to a final concentration of 20 mg·mL^{-1} by ultrafiltration on an AMICON cell with a YM10 membrane. The protein concentration was determined by measuring the UV absorbance at 280 nm using an experimental extinction coefficient of 2.2 (±0.1) cm^2·mg^{-1}. This extinction coefficient was determined by amino acid analysis at the Laboratoire de Biochimie-Ingénierie des Protéines (UMR6560, Faculty of Medicine of Marseille).

PEG 8000 (from Hampton research) and NaCl (from Sigma) were buffered to a final concentration of 50 mM Tris at pH 8.5 and prepared at 40% w/v for PEG and 2 M for salt, respectively. Protein solutions for SAXS experiments and phase-diagram determination were performed at air-conditioned room temperature (20° C). All solutions were filtered on 0.45-μm Millex-LCR filters (from Millipore).

2.2. Crystallization Trials and Phase Diagram. The crystallization trials were performed in an air-conditioned room (20 °C) with the Microbatch technique. Droplets were prepared by mixing 3 μL of a purified and concentrated urate oxidase solution with 3 μL of a precipitant agent (PEG 8000) and were pipetted under a layer of paraffin oil (paraffin oil and 72-well Microbatch plates from Hampton Research). Crystals were observed with a Nikon TE 200 microscope equipped with Nikon Plan Fluor 10× and 20× objectives. Photographs were taken with a Panasonic camera attached to the microscope and coupled to a computer and were recorded with Replay software developed by Microvision.[43]

The solubility, defined as the concentration of protein in solution in equilibrium with a crystal, was determined by seeding a supersaturated solution of urate oxidase (between 100 and 200 μL) with crushed microcrystals. PEG concentrations were between 4 and 10% w/v, and the buffer was 50 mM Tris at pH 8.5 with 100 mM NaCl. A small amount of salt was added to screen possible variations of the protein charge, eventually due to slight variations of the Tris buffer pH with temperature. The urate oxidase concentration was followed by measuring UV absorbance at 280 nm over several weeks until equilibrium was reached. Phase separations were studied without any preliminary seeding for PEG concentrations between 8 and 19% w/v. Before any crystallization event, the solution was centrifuged to determine the concentration of urate oxidase and PEG in each phase. The urate oxidase concentration in the light or the protein-poor phase (supernatant) was measured by UV absorption, and the PEG percentage was determined with an ABBE refractometer. The volume of the heavy or protein-rich phase was too small and the solution too viscous to allow accurate determinations of PEG and protein concentrations.

2.3. X-ray Scattering Experiments. Urate oxidase solutions for SAXS experiments were prepared by mixing appropriate amounts of protein and PEG 8000 stock solutions to obtain about 100 μL of urate oxidase at 13 mg·mL^{-1} in 50 mM Tris buffer at pH 8.5 and different percentages of PEG 8000. In these samples, sodium chloride was not added in order to prepare samples with higher protein and PEG concentrations. Very few differences on the PEG/Uox phase behavior were observed with or without salt addition.

X-ray scattering intensities were recorded with the D24 small-angle scattering instrument using the synchrotron radiation emitted by the storage ring DCI at LURE (Orsay). The instrument, the data acquisition system, and the thermostated cell under vacuum used for these experiments have already been described.[44−46] The wavelength of the X-rays was 1.488 Å (K edge of Ni). The sample-to-detector distance used in the phase-transition experiments was 2139 ± 5 mm yielding an s increment per channel of 1.90 ± 0.01 × 10^{-4} Å^{-1}·chnl^{-1}. From 2 to 8 frames with a duration of 100 s were recorded for urate oxidase depending on the concentration and for corresponding buffers. Curves were scaled to the transmitted intensity and subtracted from the appropriate buffer. The temperature of the cell was fixed at 20 °C.

The total concentration-normalized intensity $I(c, s)$ scattered by a solution of monodisperse spherical particles at a scattering angle of 2θ can be expressed as a function of the particle concentration c and the modulus of the scattering vector $s = 2\lambda^{-1} \sin \theta$ by

$$I(c, s) = I(0, s)\cdot S(c, s) \tag{1}$$

$I(0, s)$, the intensity scattered by one particle and usually called the particle form factor, is the Fourier transform of the spherically averaged autocorrelation function of the electron density contrast associated with the particle. The form factor is generally obtained from curves recorded at low concentrations to avoid interaction effects. $S(c, s)$, usually called the solution structure factor, is the Fourier transform of the spherically averaged autocorrelation function of the particle distribution determined by interaction pair potentials.

In a Uox−PEG binary mixture, the total scattering intensity can be written as[42]

$$I_{\text{total}}(s) = I_{\text{PEG}}(s) + I_{\text{PEG-Uox}}(s) + I_{\text{Uox}}(s) \tag{2}$$

where $I_{\text{Uox}}(s)$ is the intensity scattered by the protein particles, $I_{\text{PEG}}(s)$ is the intensity scattered by the polymer particles, and $I_{\text{PEG-Uox}}(s)$ is the so-called cross term. By analogy to a monodisperse mixture, $I_{\text{Uox}}(s)$ can be expressed as

$$I_{Uox}(s) = c_{U_{ox}} \cdot I^0_{U_{ox}}(s) \cdot S_{U_{ox}-U_{ox}}(s) \quad (3)$$

where c_{Uox} is the protein concentration, $I^0_{Uox}(s)$ is the protein form factor, and $S_{Uox-Uox}(s)$ is the protein structure factor. $I_{PEG}(s)$ and $I_{PEG-Uox}(s)$ are not strictly negligible in front of $I_{Uox}(s)$ for high protein and polymer concentrations. In our experiments, the scattering intensity $I(s)$, equal to the total intensity $I_{total}(s)$ subtracted by the intensity scattered by the solvent [i.e., the protein-free PEG solution, $I^o_{PEG}(s)$], has been plotted as a function of the scattering vector s. If we consider that the intensity scattered by PEG particles in the protein/PEG binary mixture is equal to the scattered intensity of a protein-free PEG solution at the same PEG concentration ($I_{PEG}(s) \cong I^o_{PEG}(s)$), then we can write

$$I(s) = I_{total}(s) - I^o_{PEG}(s) \cong I_{total}(s) - I_{PEG}(s) \quad (4)$$

and therefore from eq 2

$$I(s) = I_{PEG-Uox}(s) + I_{Uox}(s) \quad (5)$$

Consequently, $I(s)$ takes into account not only the intensity scattered by the protein molecules but also the cross-term intensity. Numerical treatments predict that for high protein and PEG concentrations $I_{PEG-Uox}(s)$ can be equal to about 15 to 20% of $I_{Uox}(s)$.[42,47] The PEG signal $I_{PEG}(s)$ is equal to about 5−15% of the total intensity $I_{total}(s)$ depending upon the PEG concentration.

3. Results and Discussion

3.1. Experimental Phase Diagram. Figure 1 shows the urate oxidase experimental phase diagram determined in the particular case of PEG 8000 at pH 8.5 (50 mM Tris buffer with 100 mM NaCl) and 20 °C (an air-conditioned room). The protein solubility decreases when PEG is added, as was already observed with some other proteins.[48−51] Variations of the urate oxidase solubility are similar to variations of the second virial coefficient when PEG is added. This result enhances the correlation, which has already been shown experimentally and theoretically,[14,19,52] between the solubility and the second virial coefficient.

In this phase diagram, the LLPS is metastable with respect to the solid−liquid phase separation for PEG concentrations between 4 and 10% w/v. For PEG concentrations between 8 and 10% w/v and for a Uox concentration of 14 mg·mL^{-1}, the LLPS clearly precedes the crystallization process, but the final equilibrium state corresponds to crystals surrounded by a single liquid phase. (See section 3.4 for details.) Beyond a PEG concentration of 10%, it was impossible to characterize accurately by optical microscopy the thermodynamically stable phase because at equilibrium the dense phase is too turbid.

It is well known in the colloid field that in a protein (or colloid)−polymer mixture the ratio R_g/R, where R_g is the polymer radius of gyration and R is the protein (or colloid) radius, controls the general features of the phase diagram and in particular the stability of the liquid−liquid transition toward the solubility curve.[27,31,32] In the case of an ideal dilute polymer solution, theory predicts that the liquid−liquid phase transition becomes stable if the ratio R_g/R is larger than 0.3.

In our case, the PEG 8000 radius of gyration is $R_g \approx 35$ Å,[37,42] and the protein radius is $R \approx 35$ Å.[42] The ratio R_g/R being therefore close to 1, we should have expected the LLPS to be stable in a certain domain of the urate oxidase/PEG phase diagram. Our experimental result suggests that the simple theoretical model used to predict the colloid/polymer phase diagram is not efficient in the case of protein/PEG mixtures. This discrepancy could have been expected for two major reasons. First, in most of our samples, the PEG solution is semidilute (not dilute) because its percentage is higher than the critical percentage, which is approximately 5% for the PEG 8000 Da.[53] Moreoever, PEG solutions are not ideal: we have shown in a previous paper[42] that a nonnegligible repulsive interaction can exist between polymer molecules.

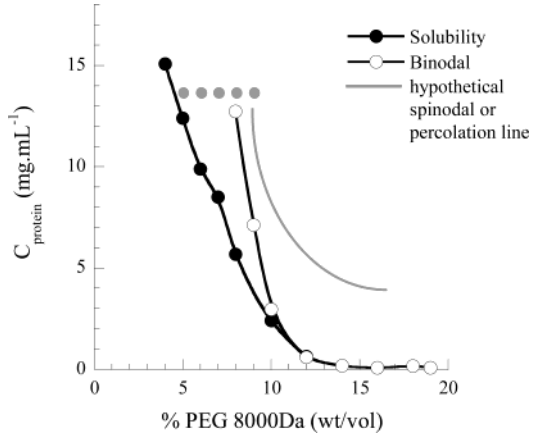

Figure 1. Phase diagram of urate oxidase in PEG 8000, 50 mM Tris buffer at pH 8.5, 100 mM NaCl with the solubility curve (solid circles), and the dilute part of the liquid−liquid phase separation (open circles); solid gray circles represent observations made by optical microscopy (Figures 2 and 6).

3.2. Characterization of Phase-Separation Morphologies by Optical Microscopy. Liquid−liquid phase-separation morphologies have been characterized by optical microscopy as a function of % PEG at a fixed urate oxidase concentration of 13.6 mg·mL^{-1} without preliminary seeding (Figure 2). The highest PEG concentration studied was 9% because of the solution turbidity.

In agreement with the experimental phase diagram (Figure 1), the LLPS is observed from a PEG 8000 concentration of 8% w/v (50 mM Tris buffer at pH 8.5 with 100 mM NaCl) and appears under the shape of disconnected droplets of several micrometers, which grow and coalesce with time. These droplets are protein-rich, the solution outside the droplets being diluted in protein. The droplet morphology characterizes a typical nucleation-and-growth mechanism, which appears for small quenches in the phase diagram between the binodal and the spinodal curves.[54,55] The nucleation-and-growth mechanism is close to the crystallization mechanism. The system is stable to small concentration fluctuations unless the droplets exceed a certain critical size. Once a droplet larger than the critical radius is formed, it keeps growing first by feeding from the external solution and then by Oswald ripening or coalescence or both.

With an addition of 9% w/v PEG 8000, the structure of the solution is totally different. The texture looks like a bicontinuous network that seems to contract itself with time, the protein-rich phase being inside the network. Such a morphology can be linked to the second mechanism—the spinodal decomposition—generally observed in the case of LLPS. It occurs for deeper quenches in the phase diagram inside the spinodal curve, where concentration fluctuations grow spontaneously. This bicontinuous morphology can also result from a percolation (or gelation) transition giving rise to a space-filling network of aggregated particles. In some colloid−polymer mixtures, it has been observed that both mechanisms are intimately linked, the percolation transition resulting from a spinodal decomposition.[56]

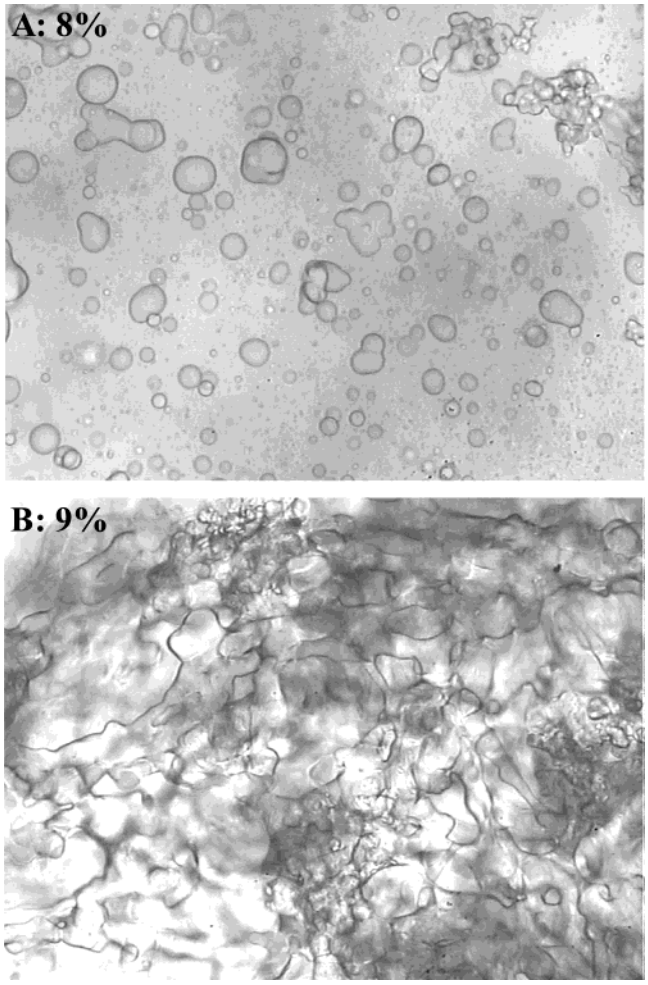

Figure 2. Optical microscopy observations of LLPS with urate oxidase 13.6 mg·mL^{-1}, 50 mM Tris buffer at pH 8.5, and 100 mM NaCl in PEG 8000: 8% (A) and 9% w/v (B). Dimensions of images are 220 × 165 μm^2.

In both cases (c_{PEG} = 8 and 9%), within minutes to hours, the dense, turbid phase slowly sediments under gravity, and the mixture separates into two phases. These two LLPS structures have already been observed with several colloid−polymer mixtures.[55−58]

3.3. Characterization of Liquid−Liquid Phase Separations by SAXS Experiments. In previous studies with two other protein/PEG systems—ATCase[15] (molecular mass = 306 kDa) and α-crystallin (molecular mass = 900 kDa) (Finet (ESRF, Grenoble) and Tardieu (LMCP, Paris), unpublished results)—LLPS was observed by SAXS experiments, but the different phases were not completely characterized. In the present work, we have coupled SAXS experiments and numerical treatments to characterize the liquid−liquid phase separation in order to get some additional information about the composition and the structure of the protein-poor and the protein-rich phases and moreover to determine the interactions between proteins in each phase. This method was successfully used in our previous work[41,42] with homogeneous Uox/PEG mixtures to determine the attractive depletion potentials between proteins induced by PEG addition.

a. LLPS and X-ray Scattered Intensity. Experiments have been performed in 50 mM Tris buffer at pH 8.5 with PEG 8000. The initial protein concentration was fixed to 13 mg·mL^{-1}. PEG concentrations from 5 to 14% have been studied.

In Figure 3, scattering intensities $I(s)$ are plotted as a function of the percentage of PEG 8000 as well as the ratio $I(s)/I_0(s)$, where $I_0(s)$ is the intensity scattered by the protein solution without PEG. All of the curves as a function of various PEG concentrations superimpose at large angles $s > 0.017$ Å^{-1} (Figure 3a and c), indicating that the number of protein particles under the X-ray beam remains the same. In other words, whatever the initial PEG concentration, no decantation occurs during SAXS experiments. Under our experimental conditions, below 9% PEG 8000, the scattering intensity increases at low angles with PEG addition (Figure 3b), which characterizes an increase in the attractive depletion interactions between proteins. These results are in agreement with previous experiments performed for lower PEG 8000 concentrations (≤5% w/v).[41,42] From 9% w/v PEG 8000, the LLPS can be visually observed: the sample becomes turbid. Note that during the determination of the experimental phase diagram (see sections 3.1 and 3.2), for a similar initial protein concentration, LLPS occurs from 8% w/v PEG 8000. This slight difference is likely due to the small amount of NaCl added in crystallization trials. (See Materials and Methods sections 2.2 and 2.3.)

The scattering curves display three general trends: the scattering intensity (Figure 3a and c) drastically increases at very low angles ($s < 0.003$ Å^{-1}) and decreases at the intermediate angles (0.003 Å^{-1} < s < 0.012 Å^{-1}), and a strong correlation peak appears around $s \approx 0.015$ Å^{-1}. These trends are much more intense than the PEG concentration is high. The same variations including the peak position have been observed with two others PEGs—PEG 3350 and PEG 20000 (data not shown).

Moreover, whatever the urate oxidase or PEG concentrations are, the LLPS is a reversible phenomenon because by the dilution of PEG (respectively protein) at constant protein (respectively PEG) concentration a homogeneous, clear phase reappears. This optical observation has also been confirmed by SAXS (data not shown). Reversible liquid−liquid phase separations were characterized with various biological systems (lysozyme, γ-crystallin, and BPTI) studied in salt as a function of temperature.[59−61]

b. Characterization of the Light and Heavy Phases. To study the dense and the dilute phases by SAXS, Uox/PEG cloudy samples were centrifuged. The intensity scattered by the supernatant was recorded, and by difference from the signal of the whole (demixed solution) mixture, we could get the intensity scattered by the dense phase. The example of 13 mg·mL^{-1} urate oxidase, 14% w/v PEG 8000 is illustrated in Figure 4a. We can see that the scattering intensity at intermediate angles is essentially due to the light phase and its decreasing intensity (Figure 3a) when PEG concentration increases, resulting from the fact that the light phase becomes poorer and poorer in protein. The correlation peak at 0.015 Å^{-1} characterizes the protein-rich phase and represents a dense, strong repulsive phase. The peak position refers to protein−protein correlations for a characteristic interprotein distance d roughly given by $d \approx 1/s_{peak}$. In our case, this distance is equal to 1/0.015 ≈ 67 Å, a value close to the protein diameter of $\sigma \approx 70$ Å. This means that in the dense phase proteins are almost stuck to each other. The peak intensity increases with the increase in PEG concentration (Figure 3c) because the dense phase is more and more concentrated in protein and consequently protein correlations are enhanced. The large increase in the intensity, which appears at very small angles ($s < 0.003$ Å^{-1}) will probably be due to the dense phase or to the LLPS itself; this will be discussed further.

In Figure 4b, we have plotted the intensity scattered by the dilute phase, normalized to the protein form factor and to the

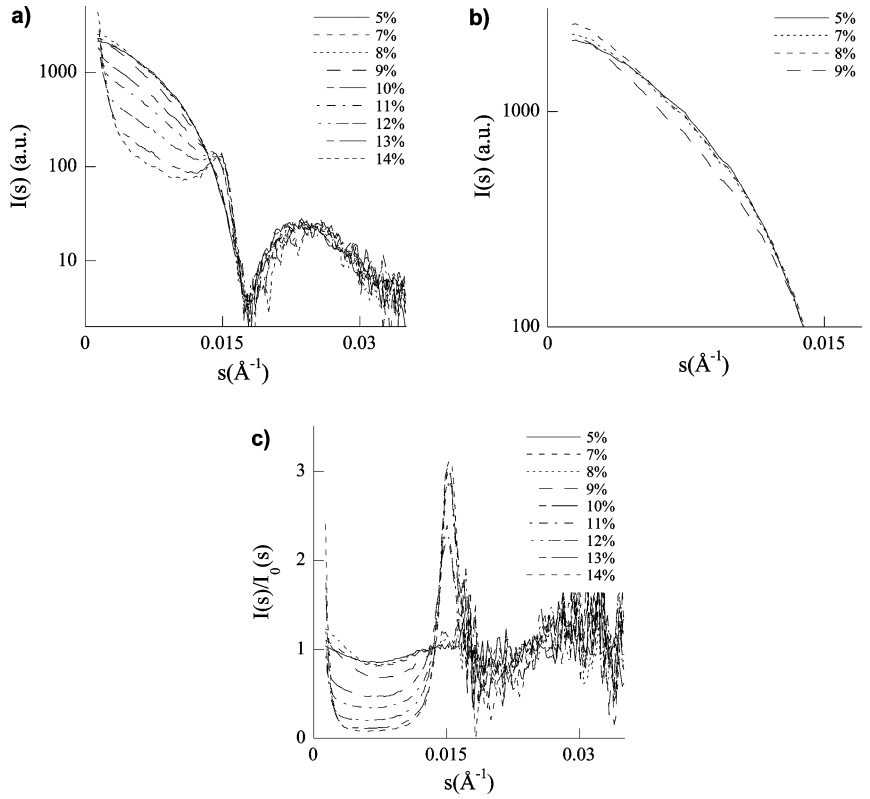

Figure 3. (a) Scattering intensities of urate oxidase (13 mg·mL^{-1}) in 50 mM Tris buffer at pH 8.5 as a function of % PEG 8000. (b) Enlargement of the small-angle zone relative to part a. (c) Scattering intensities of urate oxidase as a function of % PEG versus the polymer-free protein intensity for PEG 8000.

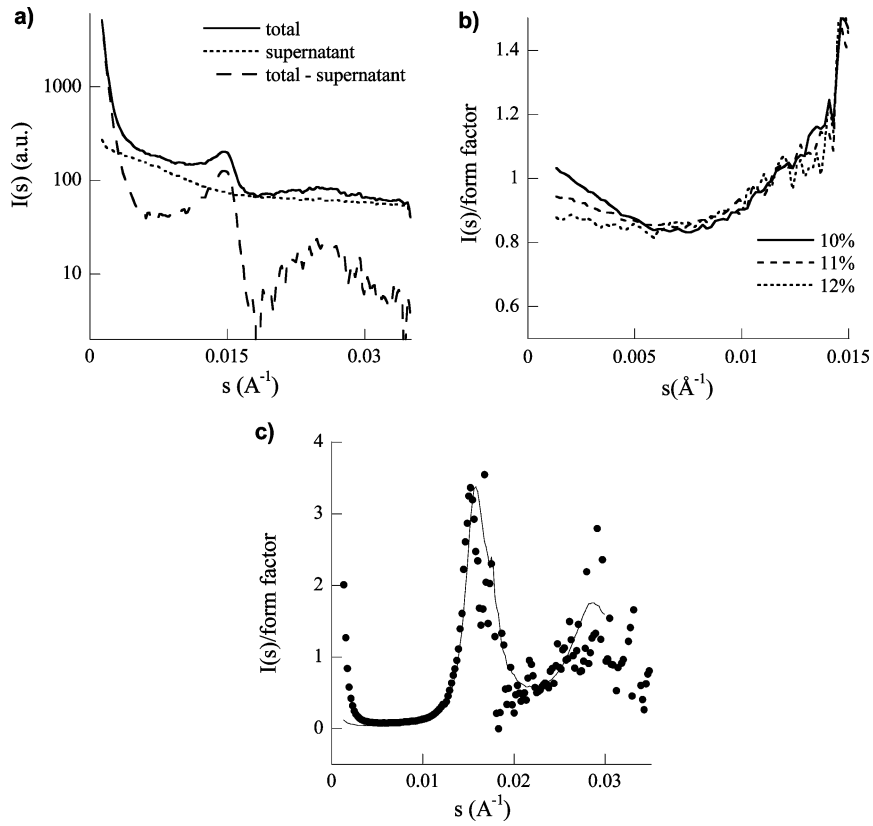

Figure 4. (a) Scattering intensity of urate oxidase (13 mg·mL^{-1}) in 14% PEG 8000 and 50 mM Tris buffer at pH 8.5. The solid line represents the scattering intensity of the demixed sample, the dotted line is the scattering intensity of the supernatant after centrifugation, and the dashed line is the signal obtained by subtracting the supernatant signal from the total signal. (b) Scattering intensity of urate oxidase supernatant/PEG 8000 versus protein form factor normalized to the protein concentration (50 mM Tris at pH 8.5). (c) Experimental (solid circles) and theoretical (straight line) scattering intensity of the dense phase versus the protein form factor. This theoretical intensity is calculated from the two-component model.

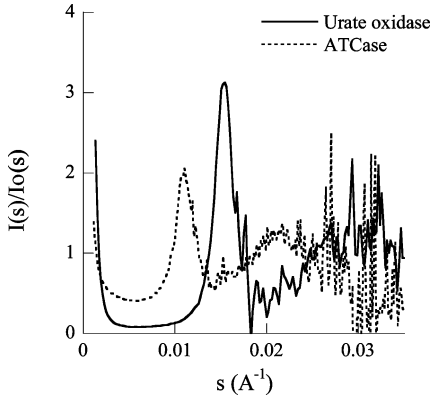

Figure 5. Scattering intensity of protein−PEG 8000 mixtures versus polymer-free protein intensity for urate oxidase (14% PEG 8000, c_{urate} = 13 mg·mL^{-1}, 50 mM Tris at pH 8.5) and ATCase (10% PEG 8000, 100 mM sodium acetate, c_{ATCase} = 30 mg·mL^{-1}, 10 mM sodium borate at pH 8.3).[15]

protein concentration, which corresponds to the protein structure factor if we consider as a rough approximation the fact that the cross term $I_{PEG-Uox}(s)$ is negligible in front of $I_{Uox}(s)$ (i.e., $I(s) \approx I_{Uox}(s)$; see Material and Methods section 2.3). In the presence of 10% w/v PEG 8000, the structure factor at low angles increases and is larger than 1, which indicates that depletion attractive interactions are present between protein molecules. The decrease of the structure factor at low angles when increasing the polymer concentration is linked to a lower protein concentration. The fact that the structure factors in the presence of 11 and 12% w/v PEG 8000 are below 1 at low angles, and not above 1 as expected because of the presence of depletion attractive interactions, is probably due to the (negative) cross term $I_{PEG-Uox}(s)$ that we have neglected.

As mentioned in Materials and Methods, because of its low volume and its viscosity, it was not possible to determine the protein and PEG concentrations accurately in the dense phase. To get some information about these concentrations, we have fit the experimental scattering intensities with the so-called "two-component" model (Figure 4c). From this numerical model, which takes into account the protein−protein, protein−polymer, and polymer−polymer pair interaction potentials,[42] theoretical scattering intensities can be calculated and then compared to the experimental intensities. The parameters of the three potentials were kept identical to those used in previous work done on urate oxidase/PEG homogeneous mixtures;[42] in particular, below 1% w/v PEG 8000, the polymer−polymer interaction was negligible. The protein and polymer concentrations were the only free parameters. This model is efficient below the critical polymer concentration,[42] equal to approximately 5% for PEG 8000 Da. We have thus studied the dense phase for the case of 13 mg·mL^{-1} urate oxidase, 14% w/v PEG 8000, the highest protein and PEG concentrations investigated. According to the Uox/PEG phase diagram, these conditions are well inside the LLPS, and the PEG concentration in the dense phase is the lowest among those from all of the samples that were studied. We succeeded in fitting the experimental structure factor with a protein volume fraction of 55% and a polymer concentration of 0.8%, which confirms that the polymer concentration in the dense phase is very low (Figure 5). The protein concentration in this phase is very high and close to the protein concentration in the crystalline phase. We cannot therefore exclude the fact that proteins are not aggregated in the dense phase. Furthermore, even if there is an increase at the very low angles of the theoretical scattering intensity, this effect is very weak in comparison with the experimental effect. As a consequence, the two-component model seems to exclude the fact that in urate oxidase/PEG mixtures the drastic increase of the scattering intensity at very low angles is due to the dense phase itself. This increase might instead come from the liquid−liquid phase separation itself and therefore from the droplets or bicontinuous network formations. We intend to perform additional experiments, in particular, light scattering and USAXS (ultrasmall-angle X-ray scattering) experiments, to try to discriminate between the different hypotheses. Recently, it has also been proposed that because of the depletion attractive interaction, reversible adhesive clusters or aggregates of particles and corresponding voids could be formed in the dense phase leading to this sharp increase in the scattering intensity.[62,63]

c. Comparison with Another Biological System. We have compared urate oxidase (molecular mass = 128 kDa) with ATCase[15] (molecular mass = 306 kDa), another protein/PEG system that has been studied by SAXS under LLPS conditions. We have reported (Figure 5) for the ATCase and urate oxidase in the presence of PEG 8000, the ratio $I(s)/I_0(s)$, where $I(s)$ is the intensity scattered by the protein/PEG mixture and $I_0(s)$ the intensity scattered by the polymer-free protein solution. The two curves look very similar and present a strong correlation peak, a decrease in intensity in the medium angles, and a drastic increase in intensity at very low angles. The main difference between them is the position of the correlation peak. Indeed, for urate oxidase ($\sigma \approx 70$ Å), it is at 0.015 Å^{-1}, and for ATCase ($\sigma \approx 120$ Å) it is at 0.0109 Å^{-1}, which corresponds to characteristic interprotein distances of 65 and 92 Å, respectively. This evolution is expected because in the dense phase proteins are really stuck to each other; consequently, a protein is larger and the characteristic interproteic distance should be longer in the dense phase. We can observe that the characteristic interprotein distances are shorter than the protein diameter, and they are expected to be slightly superior. One possible reason is that the relation $d \approx 1/s_{peak}$ gives only an indication of the interparticle distance in the dense phase.

This comparative study shows that our results are not specific to the Uox/PEG system and can be generalized to other protein/polymer systems.

3.4. Implications for Protein Crystallization. To see the LLPS influence on crystallization or crystal growth mechanisms, we have performed some time-lapse crystallization experiments after seeding different Uox/PEG mixtures in different regions of the protein phase diagram (Figures 6). The microseeding technique[64] was used so that no crystal was visible under the microscope at time zero. Seeding our samples was necessary to avoid the primary nucleation step, which is difficult to control and to reproduce. We thus observed the homogeneous growth of the seeded crystals and/or of secondary nuclei. We have investigated the time until crystals were detectable by optical microscopy (approximately with a size greater than 10 μm). It is important to notice that the following results do not depend on the original crystal habit of the seeded crystals. The protein concentration was fixed to 13.6 mg·mL^{-1}, and the PEG concentration varied between 5 and 9% w/v. Between the solubility and the LLPS curves ($5\% \leq c_{PEG} \leq 7\%$), the crystallization occurs as expected without any liquid−liquid phase separation (Figure 6a−f). Different crystal habits were observed depending upon the PEG concentration; their morphological description and their crystallographic characterization will be discussed elsewhere (Vivarès et al, in preparation). We have, for instance, proven that the massivelike crystals (observed with $c_{PEG} = 5\%$) and the needlelike crystals (observed with $c_{PEG} = 6\%$) are the same polymorph whereas the platelike crystals

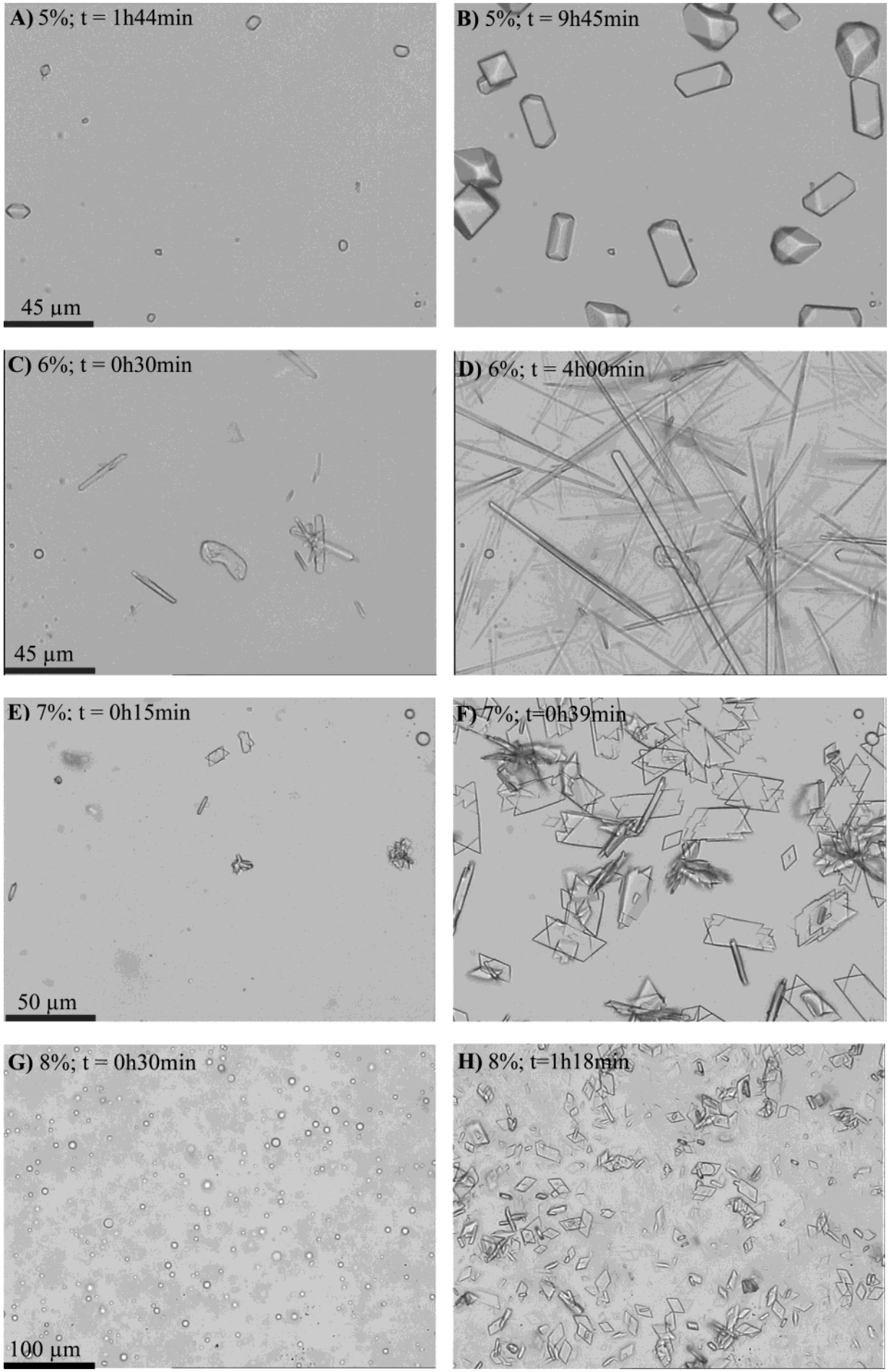
A) 5%; t = 1h44min
45 µm
B) 5%; t = 9h45min
C) 6%; t = 0h30min
45 µm
D) 6%; t = 4h00min
E) 7%; t = 0h15min
50 µm
F) 7%; t=0h39min
G) 8%; t = 0h30min
100 µm
H) 8%; t=1h18min

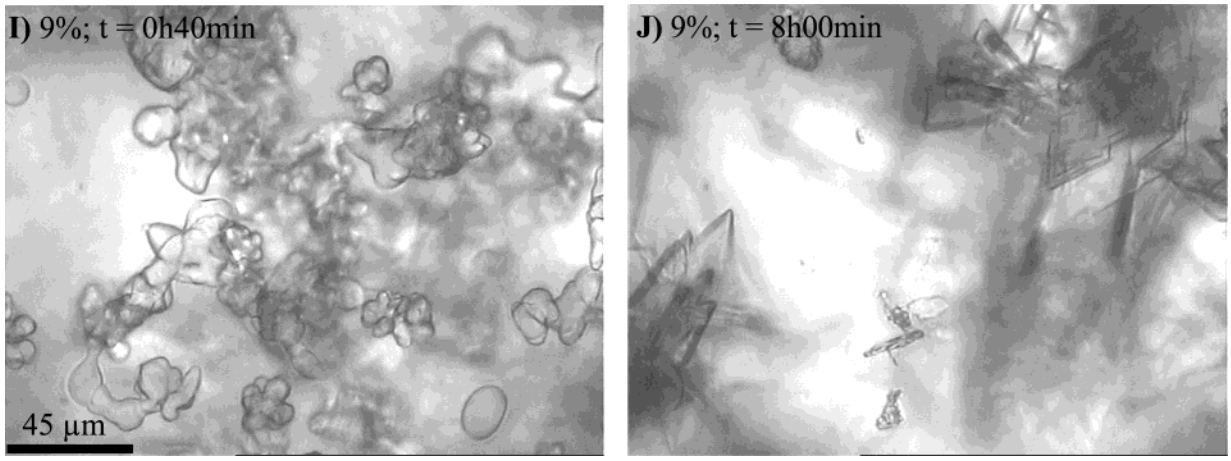

Figure 6. (A−J) Crystallization experiments of urate oxidase (13.6 mg·mL^{-1}, 50 mM Tris at pH 8.5, 100 mM NaCl) performed by seeding on both sides of the liquid−liquid phase boundary (solid gray circles of Figure 1) in 5, 6, 7, 8, and 9% w/v PEG 8000 as a function of time.

(observed with c_{PEG} = 7, 8, and 9%) correspond to a different polymorph (Vivarès et al, in preparation). Beyond the LLPS curve (c_{PEG} = 8% and c_{PEG} = 9%), the formation of droplets (c_{PEG} = 8%) or the formation of a bicontinuous network (c_{PEG} = 9%) occurs before the crystallization process (Figure 6g−j). These observations are in agreement with the previous ones without any crystal seeding (Figure 2) and confirm that the crystalline phase is the equilibrium phase whereas the LLPS is the metastable one. Below the LLPS (c_{PEG} = 5, 6, or 7%), the crystallization steps are faster with increasing PEG concentration and therefore with supersaturation, which indicates that in our mixtures the crystal growth step is mainly governed by the supersaturation β (= C/C_s, where C is the protein concentration and C_s is the protein solubility). Another parameter, the increase in the solution viscosity with increasing PEG concentration, which can affect the particles' diffusion, does not seem to play an important role. Beyond the LLPS, when c_{PEG} = 8% and particularly when c_{PEG} = 9%, the crystallization is delayed in comparison with that of the lower PEG concentration samples. The behavior of Uox/PEG mixtures seems to be similar to that of the lysozyme/salt system as a function of temperature,[25] for which it was observed that the nucleation rate decreases beyond the LLPS. This decrease has been attributed to the competition between the crystallization and the nucleation of droplets.[25] However, unlike the lysozyme/salt system, in protein/PEG mixtures, solution compositions are not identical in the protein-poor and in the protein-rich phases. In our mixtures, it was not possible to distinguish by optical microscopy in which phase the nucleation and crystal growth occur. To understand the slower-than-expected crystal growth beyond the liquid−liquid phase boundary, we have to check the composition of both phases. For the sake of clarity, let us consider the sample with an initial protein concentration of 13.6 mg·mL^{-1} and an initial polymer concentration of 9%. The PEG concentration in the light phase was found to be similar to the initial PEG concentration (i.e., 9%), and the protein concentration was equal to 7 mg·mL^{-1}. Consequently, the supersaturation β in the light phase is equal to 1.8, a supersaturation higher than the ones observed with a PEG concentration of 5% (β = 1.1), 6% (β = 1.4), or 7% (β=1.6). Consequently, if the crystal growth occurs in the light phase, the slower crystal growth observed is not due to a supersaturation effect but may instead be due to the competition between the formation and growth of the bicontinuous structure and the crystal growth. The dense phase, as shown by the SAXS study, is highly concentrated in proteins with a low polymer concentration, and the protein−protein interactions are mostly repulsive. The protein volume fraction in the dense phase is close to the protein volume fraction in the crystal phase, which means that, in the dense phase, protein molecules are probably aggregated in a gellike state. Consequently, if crystal growth occurs in the dense phase, then the slower crystal growth observed can be explained either by the fact that the supersaturation is very low or more probably by the fact that the protein molecules are in an "arrested" state. This assumption can be closely linked to the cessation of crystallization reported in a colloid−polymer mixture and attributed to the presence of a metastable fluid−fluid phase separation; beyond this fluid−fluid phase separation, metastable and amorphous precipitates, aggregates, or gels are formed instead of crystals.[65,66]

4. Conclusions

The present work is aimed at studying the urate oxidase/PEG 8000 phase diagram. We have experimentally determined the solubility curve (i.e., the solid−liquid phase separation) and the binodal (or liquid−liquid phase separation). The LLPS was characterized by video optical microscopy and SAXS, and its effect on urate oxidase crystallization and crystal growth was analyzed.

We have shown that the variation of the urate oxidase solubility when PEG is added is similar to the variation of the second virial coefficient (A_2), which enhances the close correlation between solubility and A_2 and confirms that the second virial coefficient turns out to be a good predictor of protein crystallization.

We have characterized an LLPS, which is metastable toward the solubility curve over the whole PEG−protein concentration range studied. By video microscopy, we have observed two morphologies. Close to the LLPS boundary (binodal), the LLPS looks like droplets, and for deeper quenches it looks like a bicontinuous network. The droplet morphology can be associated with the so-called nucleation-and-growth mechanism whereas the bicontinuous network can be linked to the spinodal decomposition and/or to a percolation transition.

Furthermore, we have also studied the LLPS by small-angle X-ray scattering (SAXS). When the protein/PEG mixture undergoes an LLPS, the whole scattering intensity curve reveals a strong correlation peak at a fixed angle, decreasing intensity at intermediate angles, and a drastic increase at very low angles. The correlation peak characterizes a repulsive dense phase and was successfully fit with the numerical two-component model.

The fitting confirms that the protein volume fraction in the dense phase is very high whereas the PEG concentration is very low. The drastic increase at very low angles may be due to the dense phase or to the LLPS itself. Finally, the signal from the intermediate angles corresponds to that from the light phase, and its decrease is linked to the decreasing protein concentration in the light phase when the PEG concentration increases. Furthermore, in the light phase, which is supersaturated and therefore may crystallize, we have also shown that attractive interactions are present, which is expected from the high PEG concentrations.

Furthermore, we have shown that the LLPS precedes and delays the crystal growth. This is an important finding in the general context of the LLPS influence on protein crystallization. Considering that the crystallization occurs in the light or in the dense phase, we can propose two different hypotheses. If crystallization occurs in the light phase, then the competition between the formation of LLPS and the crystal growth can explain the observed delay. If crystallization occurs in the dense phase, the fact that the protein molecules are in an "arrested" gellike state can also slow the crystal growth.

In conclusion, the present study sheds new light on the effect of a metastable LLPS on protein crystallization. Moreover, this work clearly shows that the urate oxidase/PEG mixture is a suitable system for studying the morphology and the structure of colloid−polymer LLPS. SAXS experiments have also shown that this technique can give some important information about the structure of such mixtures.

Acknowledgment. We gratefully acknowledge M. El Hajji (Sanofi-Synthelabo, France) for generously providing us with urate oxidase and for his interest in this study. We thank P. Vachette and J. Perez (LURE, Orsay) for their help and their suggestions during SAXS experiments on the D24 instrument, P. Mansuelle (UMR6560, Faculty of Medicine of Marseille) for the determination of the urate oxidase extinction coefficient, L. Belloni (CEA, Saclay) for fruitful and critical discussions, and S. Veesler for critically reading the manuscript. Small-angle X-ray scattering experiments on the liquid−liquid phase separation of Uox/PEG mixtures were partially motivated by the initial work done by S. Finet (ESRF, Grenoble) and A. Tardieu (LMCP, Paris) on α-crystallin/PEG mixtures.

References and Notes

(1) Boistelle, R.; Astier, J. P. *J. Cryst. Growth* **1988**, *90*, 14.
(2) Durbin, S. D.; Feher, G. *Annu. Rev. Phys. Chem.* **1996**, *47*, 171.
(3) Rosenberger, F.; Vekilov, P. G.; Muschol, M.; Thomas, B. R. *J. Cryst. Growth* **1996**, *168*, 1.
(4) McMillan, R. A.; Paavola, C. D.; Howard, J.; Chan, S. L.; Zaluzec, N. J.; Trent, J. D. *Nat. Mater.* **2002**, *1*, 247.
(5) Lafferrère, L.; Hoff, C.; Veesler, S. *Eng. Life Sci.* **2003**, *3*, 127.
(6) Pande, A.; Pande, J.; Asherie, N.; Lomakin, A.; Ogun, O.; King, J.; Benedek, G. B. *Proc. Natl. Acad. Sci. U.S.A.* **2001**, *98*, 6116.
(7) Israelachvili, J. *Intermolecular and Surface Forces*; Academic Press: New York, 1994.
(8) Tardieu, A. *Thermodynamics and Structure*: *Concentrated Solutions − Structured Disorder in Vision*; Springer-Verlag: New York, 1994; p 145.
(9) Muschol, M.; Rosenberger, F. *J. Chem. Phys.* **1995**, *103*, 10424.
(10) Ducruix, A.; Guilloteau, J. P.; Riès-Kautt, M.; Tardieu, A. *J. Cryst. Growth* **1996**, *168*, 28.
(11) George, A.; Wilson, W. W. *Acta Crystallogr., Sect. D* **1994**, *50*, 361.
(12) Lafont, S.; Veesler, S.; Astier, J. P.; Boistelle, R. *J. Cryst. Growth* **1997**, *173*, 132.
(13) Velev, O. D.; Kaler, E. W.; Lenhoff, A. M. *Biophys. J.* **1998**, *75*, 2682.
(14) Bonneté, F.; Finet, S.; Tardieu, A. *J. Cryst. Growth* **1999**, *196*, 403.
(15) Budayova, M.; Bonneté, F.; Tardieu, A.; Vachette, P. *J. Cryst. Growth* **1999**, *196*, 210.
(16) Hitscherich, C. J.; Kaplan, J.; Allaman, M.; Wiencek, J.; Loll, P. J. *Protein Sci.* **2000**, *9*, 1559.
(17) Bonneté, F.; Vivarès, D.; Robert, C.; Colloc'h, N. *J. Cryst. Growth* **2001**, *232*, 330.
(18) Solovyova, A.; Schuck, P.; Costenaro, L.; Ebel, C. *Biophys. J.* **2001**, *81*, 1868.
(19) Demoruelle, K.; Guo, B.; Kao, S.; McDonald, H. M.; Nikic, D. B.; Holman, S. C.; Wilson, W. W. *Acta Crystallogr., Sect. D* **2002**, *58*.
(20) Tessier, P. M.; Lenhoff, A. M.; Sandler, S. I. *Biophys. J.* **2002**, *82*, 1620.
(21) Tessier, P. M.; Johnson, H. R.; Pazhianur, R.; Berger, B. W.; Prentice, J. L.; Bahnson, B. J.; Sandler, S. I.; Lenhoff, A. M. *Proteins* **2003**, *50*, 303.
(22) Muschol, M.; Rosenberger, F. *J. Chem. Phys.* **1997**, *107*, 1953.
(23) ten Wolde, P. R.; Frenkel, D. *Science* **1997**, *277*, 1975.
(24) Haas, C.; Drenth, J. *J. Phys. Chem. B* **1998**, *102*, 4226.
(25) Galkin, O.; Vekilov, P. G. *Proc. Natl. Acad. Sci. U.S.A.* **2000**, *97*, 6277.
(26) Veesler, S.; Lafferrere, L.; Garcia, E.; Hoff, C. *Org. Process Res. Dev.* **2003**, *7*, 983.
(27) Anderson, V. J.; Lekkerkerker, H. N. W. *Nature* **2002**, *416*, 811.
(28) Asakura, S.; Oosawa, F. *J. Chem. Phys.* **1954**, *22*, 1255.
(29) Vrij, A. *Pure Appl. Chem.* **1976**, *48*, 471.
(30) Gast, A. P.; Hall, C. K.; Russel, W. B. *J. Colloid Interface Sci.* **1983**, *96*, 251.
(31) Lekkerkerker, H. N. W.; Poon, W. C. K.; Pusey, P. N.; Stroobants, A.; Warren, P. B. *Europhys. Lett.* **1992**, *20*, 559.
(32) Ilett, S. M.; Orrock, A.; Poon, W. C. K.; Pusey, P. N. *Phys. Rev. E* **1995**, *51*, 1344.
(33) Kulkarni, A. M.; Chatterjee, A. P.; Schweizer, K. S.; Zukoski, C. F. *J. Chem. Phys.* **2000**, *113*, 9863.
(34) Casselyn, M.; Perez, J.; Tardieu, A.; Vachette, P.; Witz, J.; Delacroix, H. *Acta Crystallogr., Sect. D* **2001**, *57*, 1799.
(35) Finet, S.; Tardieu, A. *J. Cryst. Growth* **2001**, *232*, 40.
(36) Kulkarni, A.; Zukoski, C. F. *J. Cryst. Growth* **2001**, *232*, 156.
(37) Tanaka, S.; Ataka, M. *J. Chem. Phys.* **2002**, *117*, 3504.
(38) Tanaka, S.; Ataka, M.; Onuma, K.; Kubota, T. *Biophys. J.* **2003**, *84*, 3299.
(39) Annunziata, O.; Asherie, N.; Lomakin, A.; Pande, J.; Ogun, O.; Benedek, G. B. *Proc. Natl. Acad. Sci. U.S.A.* **2002**, *99*, 14165.
(40) Annunziata, O.; Ogun, O.; Benedek, G. B. *Proc. Natl. Acad. Sci. U.S.A.* **2003**, *100*, 970.
(41) Vivarès, D.; Bonneté, F. *Acta Crystallogr., Sect. D* **2002**, *58*, 472.
(42) Vivarès, D.; Belloni, L.; Tardieu, A.; Bonneté, F. *Eur. Phys. J. E* **2002**, *9*, 15.
(43) Boistelle, R.; Astier, J. P.; Marchis-Mouren, G.; Dessaux, V.; Haser, R. *J. Cryst. Growth* **1992**, *123*, 109.
(44) Boulin, C.; Kempf, R.; Koch, M. H. J.; McLaughlin, S. M. *Nucl. Instrum. Methods* **1986**, *A249*, 399.
(45) Depautex, C.; Desvignes, C.; Feder, P.; Lemonnier, M.; Bosshard, R.; Leboucher, P.; Dageaux, D.; Benoit, J. P.; Vachette, P. *LURE: rapport d'activité pour la période Août 1985−1987*; edited by documentation CEN Saclay, 1987.
(46) Dubuisson, J. M.; Decamps, T.; Vachette, P. *J. Appl. Crystallogr.* **1997**, *30*, 49.
(47) Vivarès, D. Interactions en solution et cristallisation de l'urate oxidase. Ph.D. Thesis, Université Pierre et Marie Curie, Paris, France, 2003.
(48) Atha, D. H.; Ingham, K. C. *J. Biol. Chem.* **1981**, *256*, 12108.
(49) Haire, R. N.; Tisel, W. A.; White, J. G.; Rosenberg, A. *Biopolymers* **1984**, *23*, 2761.
(50) Odahara, T.; Ataka, M.; Katsura, T. *Acta Crystallogr., Sect. D* **1994**, *50*, 639.
(51) Gaucher, J. F.; Riès-Kautt, M.; Reiss-Husson, F.; Ducruix, A. *FEBS Lett.* **1997**, *401*, 113.
(52) Haas, C.; Drenth, J.; Wilson, W. W. *J. Phys. Chem. B* **1999**, *103*, 2808.
(53) Vincent, B.; Luckham, P. F.; Waite, F. A. *J. Colloid Interface Sci.* **1980**, *73*, 508.
(54) Butler, M. F. *Biomacromolecules* **2002**, *3*, 676.
(55) Koenderink, G. H.; Aarts, D. G. A. L.; de Villeneuve, V. W. A.; Philipse, A. P.; Tuinier, R.; Lekkerkerker, H. N. W. *Biomacromolecules* **2003**, *4*, 129.
(56) Verhaegh, N. A. M.; Asnaghi, D.; Lekkerkerker, H. N. W.; Giglio, M.; Cipelletti, L. *Physica A* **1997**, *242*, 104.
(57) van Bruggen, M. P. B.; Dhont, J. K. G.; Lekkerkerker, H. N. W. *Macromolecules* **1999**, *32*, 2256.
(58) Verhaegh, N. A. M.; Asnaghi, D.; Lekkerkerker, H. N. W. *Physica A* **1999**, *264*, 64.
(59) Thomson, J. A.; Schurteberger, P.; Thurston, G. M.; Benedek, G. B. *Proc. Natl. Acad. Sci. U.S.A.* **1987**, *84*, 7079.
(60) Taratuta, V. G.; Holschbach, A.; Thurston, G. M.; Blankschtein, D.; Benedek, G. B. *J. Phys. Chem.* **1990**, *94*, 2140.

(61) Grouazel, S.; Perez, J.; Astier, J.-P.; Bonnete, F.; Veesler, S. *Acta Crystallogr., Sect. D* **2002**, *58*, 1560.
(62) Shah, S.; Ramakrishnan, S.; Chen, Y.; Schweizer, K. S.; Zukoski, C. F. *Langmuir* **2003**, *19*, 5128.
(63) Shah, S.; Chen, Y.; Ramakrishnan, S.; Schweizer, K.; Zukoski, C. *J. Phys.: Condens. Matter* **2003**, *15*, 4751.
(64) Stura, E. A.; Wilson, I. A. Seeding Techniques. In *Crystallization of Nucleic Acids and Proteins: A Practical Approach*; Giegé, R., Ed.: Oxford, England, 1999; p 99.
(65) Poon, W. C. K.; Pirie, A. D.; Pusey, P. N. *Faraday Discuss.* **1995**, *101*, 65.
(66) Poon, W. C. K. *Phys. Rev. E* **1997**, *55*, 3762.